Proceedings Paper:
Forbes, F., Smith, A. and Damian, D.D. (2022) Characterization of an inflatable soft actuator and tissue interaction for in vitro mechanical stimulation of tissue. In: Pacheco-Gutierrez, S., Cryer, A., Caliskanelli, I., Tugal, H. and Skilton, R., (eds.) Towards Autonomous Robotic Systems: 23rd Annual Conference, TAROS 2022, Culham, UK, September 7–9, 2022, Proceedings. 23rd Annual Conference Towards Autonomous Robotic Systems (TAROS 2022), 07-09 Sep 2022, Culham, UK. Lecture Notes in Computer Science / Lecture Notes in Artificial Intelligence, LNCS 13546. Springer International Publishing, pp. 105-113. ISBN: 9783031159077. ISSN: 0302-9743. EISSN: 1611-3349.

https://doi.org/10.1007/978-3-031-15908-4_9

Characterization of an Inflatable Soft Actuator and Tissue Interaction for In Vitro Mechanical Stimulation of Tissue*

Frederick Forbes[1], Abigail Smith[1], and Dana D. Damian[1,2][0000−0002−0595−0182]

[1] Sheffield Biomedical Robotics Lab, Automatic Control Systems Engineering Department, University of Sheffield, Sheffield, S1 3JD, United Kingdom
{fforbes2,d.damian}@sheffield.ac.uk
[2] Insigneo Institute for in silico Medicine, University of Sheffield, Sheffield, S1 3JD, United Kingdom

Abstract. Technology to improve tissue development is constantly being improved and refined. Soft robots have been utilized in medical settings due to their compliant nature, reducing the stiffness gradient at tissue-device interfaces. In this paper, we present a pneumatically actuated soft stimulating balloon capable of applying up to 70% strain to a phantom tissue construct at a pressure of 0.3 bar. Ecoflex^{TM}0050 is used as a biocompatible material for the membrane, and the interaction between the two was investigated by varying the scaffold stiffness and initial tension. Data from video tracking was used to compute the tensile strain applied to the scaffold. We present here, the first steps of characterizing the device for in vitro implementation and further integration into a custom bioreactor.

Keywords: Tissue Engineering · Soft Robotics · Mechanobiology.

1 Introduction

In the field of tissue engineering, stimulation methods are used to mimic the body's native environment for healthy production of neotissue. Different stimulation methods and regimes have been implemented to stimulate targeted cell types and encourage cell proliferation and other cell functions, such as collagen deposition [1, 2]. These methods can also increase the likelihood of achieving desired material properties, including tissue tensile strength [3]. Mechano-stimulation has been used to apply strain and induce cell action via shear [4], tensile [5] and compressive [6] stresses.

Bioreactors are commonly used to model the behaviour found in the cell's natural environment by providing a uni-directional stimulation, such as mechanical loading. Examples of rigid traditional bioreactors include Ebers [7], BioTense

* This work was partially funded by The United Kingdom Engineering and Physical Sciences Research Council grant EP/S021035/1 and by a Department of Automatic Control and Systems Engineering, University of Sheffield, PhD scholarship

[8] and Cartigen [9]. However, stiffness gradients have been shown to affect cell activity and function [10], while soft interfaces better mimic the cell environment, therefore reducing the stiffness gradient at the boundary between the tissue construct and the actuator [11]. As a consequence, it is desirable to have a highly controllable interface where the strain intensity and direction can be regulated. Soft robots are suitable for such interfaces due to their intrinsically soft construction and the ability to control their deformation. This makes them a suitable candidate for the mechano-stimulation of tissue [12].

Research has been carried out on soft bioreactors capable of stretching and compressing cells to promote growth. Elastomeric poly-dimethylsiloxane (PDMS) membranes are widely used in combination with pneumatic or hydraulic actuation to apply strain or compress cells [13–15]. Liu et al. [16, 17] also demonstrated a PDMS and hydrogel composite that combines stretch and compression, and integrates tissue stiffness measurements. Flexcell Inc have also developed commercially available bioreactors that exert strain by using a vacuum on rubber membrane microwells [18]. Finally, other methods of actuation of elastomeric membranes include work on pin-actuated flexible membranes for stretching by Kamotani et al. [19].

Most soft stimulation devices presented in the literature demonstrate the capability of stimulation from a single source. However, our aim is to add multi-directional stimuli using different sources. In [20], our group presented a robotic bioreactor equipped with stiffness-based control to stimulate tissue constructs. This is capable of providing a tensile strain by moving the clamps apart. This work presents a soft ballooning actuator that can be integrated into the previously developed bioreactor. It is able to apply a controllable strain to a tissue construct to increase the tensile stimulation modalities and directions. A concept illustration for this is shown in Figure 1.

2 Methodology

The following section presents the design of the stimulating balloon, the manufacturing protocol for soft matter, the experimental set-up and procedure.

2.1 Stimulating Balloon Design and Integration into Bioreactor Chamber

The stimulating balloon required specific design parameters to ensure: 1) the materials exposed to cells are biocompatible, 2) controllable tensile strains can be applied to a tissue scaffold, 3) the actuator can be integrated with the current bioreactor for future combined stimulation regimes and 4) the chamber that houses the cells must be isolated from the external environment and able to be sterilized.

An exploded view diagram of the stimulating balloon is shown in Figure 2. The assembly consists of a 1mm thick membrane, secured using a cap with a

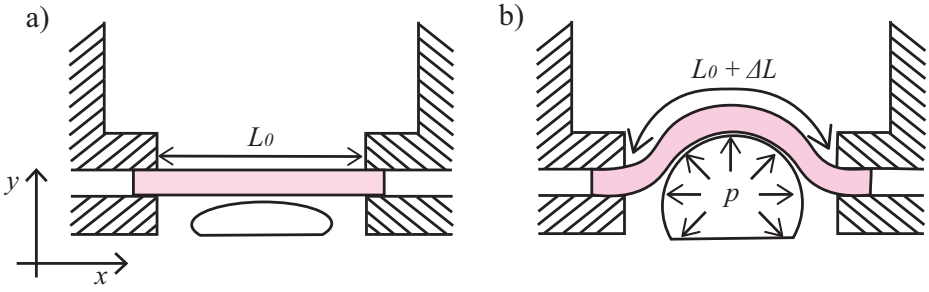

Fig. 1. Illustration of the presented stimulation method. The pink shaded area represents the tissue scaffold seeded with cells, the hatched area represents the clamps that hold the tissue scaffold in place and below is the ballooning membrane. a) When no stimulation is applied , L_0 is the length of the scaffold fixed between the two clamps, b) When the stimulating balloon is pressurized, p increases and causes the actuator to expand. The tissue scaffold is stretched, and the length increases by ΔL, representing a tensile strain.

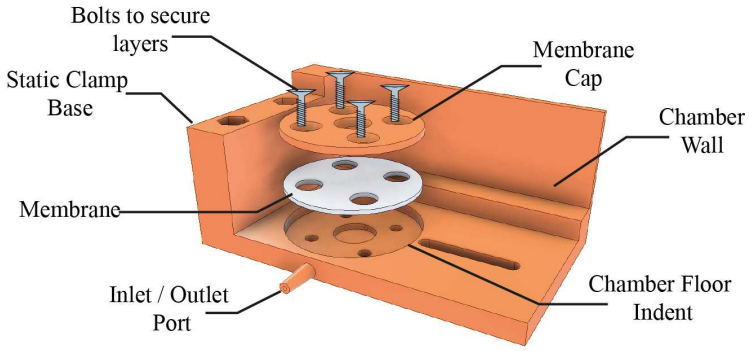

Fig. 2. Exploded-view diagram of the stimulating balloon assembly.

10mm diameter central hole to allow the membrane to balloon out when pressurized. The membrane is made of Ecoflex^{TM}0050 (E50) (Smooth On Inc.), chosen for its biocompatibility [21], and is fabricated using the procedure described in the following section. The bioreactor floor and membrane cap are 3D printed (Formlabs Form 2) using clear resin.

Finally, the ballooning membrane is inflated and monitored via two 1mm diameter channels connecting a syringe pump and pressure sensor to the pneumatic chamber.

2.2 Soft Matter Fabrication

To make the phantom scaffolds, Ecoflex^{TM}0030 (E30) (Smooth On Inc.), E50 and Moldstar^{TM}15 SLOW (MS15) (Smooth On Inc.) are combined in equal

quantities with their respective A and B parts and mixed in an ARE-250 mixer (Thinky) for three minutes. Next, they were degassed and poured into durable resin moulds (Formlabs Form 3) and left to cure at room temperature. 10mm × 20mm × 1mm scaffolds were moulded with a central row of small nodes (0.5mm deep, 1mm diameter) to allow tracking of different points during pressurization of the stimulating balloon. Three scaffolds for each material were made. Ballooning membranes were also made with E50, following the above procedure using a membrane mould.

2.3 Stimulating Balloon Experimental Set-up and Procedure

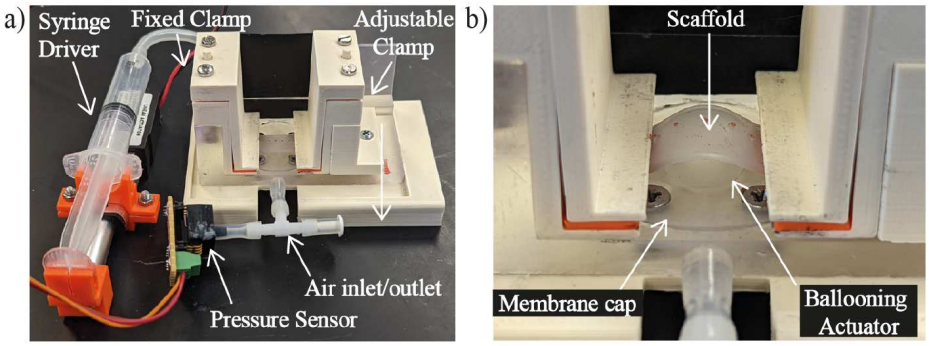

Fig. 3. a) Labelled images of the stimulating balloon experimental setup. b) Close-up labelled image of the scaffold and ballooning actuator.

An Arduino Nano was used to control a syringe driver which utilised a 12V linear actuator (Amazon) and a motor driver (Sparkfun). A pressure sensor (Honeywell) was used to measure the pressure within the chamber. Close-up videos of the scaffold were captured using a microscope camera.

A scaffold was held in place above the membrane using one fixed and one adjustable 3D-printed clamp (Prusa i3 MK3), to accommodate different scaffold lengths and apply tension, as shown in Figure 3. The pressure was then increased from 0 bar to 0.3 bar and decreased back to 0 bar in set increments. Each target pressure was held for two seconds and then updated. For each scaffold five cycles were captured.

The videos were imported to Tracker, a video tracking software. This was used to record the x and y coordinates of the nodes on the scaffold and the clamps in time, as shown in Figure 4. Using the coordinates, the length between each node pair was calculated and summed to calculate a total scaffold length, L_t. The length of the scaffold at 0 bar was set as the original length, L_0. The change in length, was used to calculate the maximum percentage strain, ϵ, as shown in Eq.1

$$\epsilon = (L_t - L_0)/(L_0 \times 100) \tag{1}$$

Finally, linear interpolation is used to determine the strain at the recorded pressures. The data from the five cycles for each scaffold were averaged. For the strain, the data is shown as the median and the error bars show the 95% confidence interval. For the pressure, the mean value is plotted and the error shown is the standard deviation.

Different elastomers were chosen for their varying stiffness; E30, E50 and MS15. The Young's modulus for the materials used in this experiment were derived using a uniaxial tensile test machine (IMADA MX2) and are shown in Table 1.

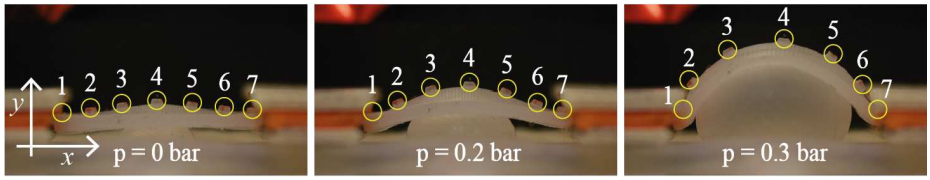

Fig. 4. Video stills of the stimulating balloon inflation at 0 bar, 0.2 bar and 0.3 bar. Yellow circles highlight the nodes that were recorded in Tracker.

Table 1. Young's Modulus for each phantom scaffold material

Material	Young's Modulus (kPa)
Ecoflex^{TM}0030	40
Ecoflex^{TM}0050	120
Mold Star^{TM} 15 SLOW	410

Different pre-strains were applied to the scaffold and tested. The pretension of an E50 scaffold was varied by changing the distance between the clamps. For 0% strain, the scaffold was fixed and the clamp adjusted until the scaffold was just in tension. Using the initial length measured as the distance between the clamps, a new distance for each strain is calculated and the clamps adjusted. The distance between the clamps were measured and changed to apply 0, 5, 10 and 20% strains.

3 Results and Discussion

The results for how the strain is affected by 1) changing the stiffness of the phantom scaffold and 2) the pre-tension of the scaffold are presented here.

Figure 5 shows that by increasing the stiffness of the phantom scaffold material, this decreases the strain that the stimulating balloon applies for given pressure. E30 and E50 scaffolds demonstrate hyperelastic behaviour, shown by

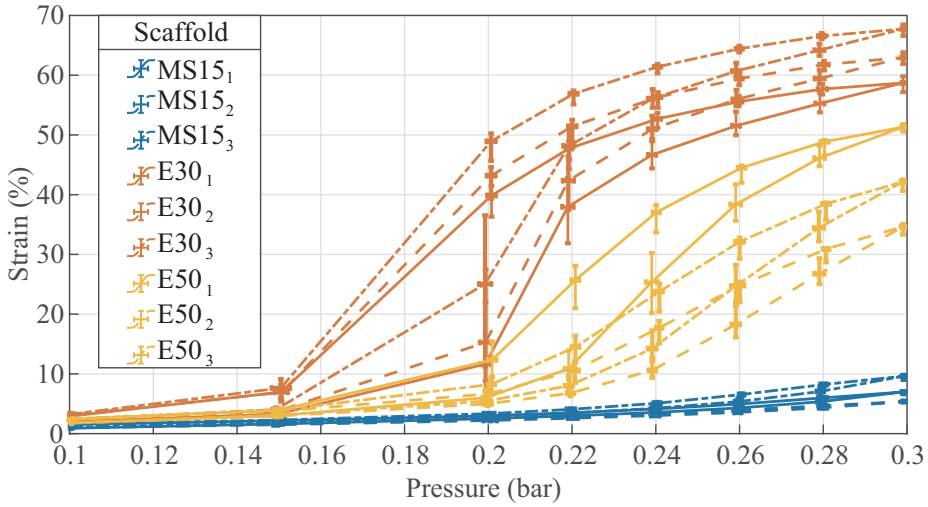

Fig. 5. The relationship between strain and pressure for different scaffold materials. This shows how the stiffness of the material changes the strain applied by the balloon. The materials used are MS15, E30 and E50.

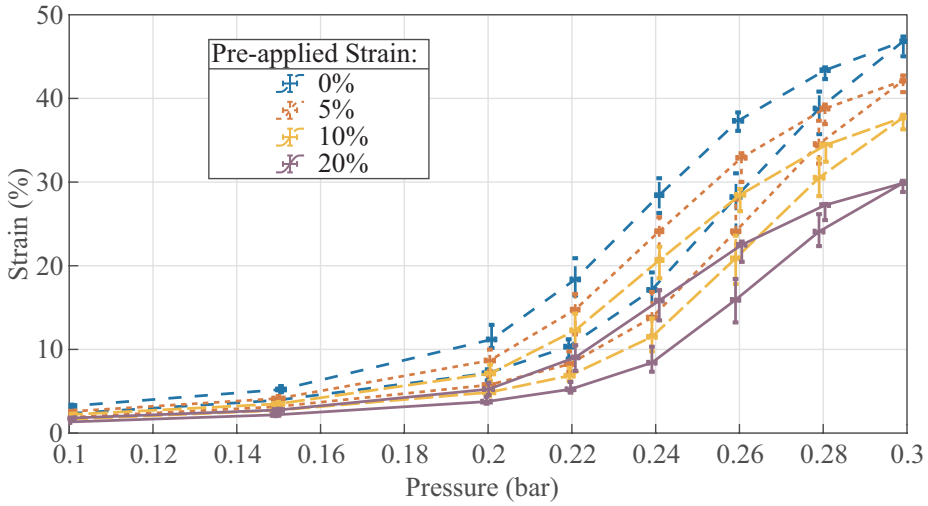

Fig. 6. The relationship between strain and pressure for various pre-tension values (0, 5, 10 and 20%) of an E50 scaffold. This shows how the initial tension applied to the phantom scaffold affects the strain produced by the balloon.

the characteristic hysteresis curves. At 0.3 bar, the average maximum strain achieved for the E30, E50 and MS15 scaffolds were approximately 63, 43 and 7%, respectively. The results show hysteresis; within each hysteretic loop, infla-

tion describes the lower half of the cycle and deflation is the top half. There is a large variation within samples of the same material, although they all follow the same trend. This could be due to how the scaffold was positioned, whether the tension was equal or due to manufacture variability e.g. slight differences in thickness. The error in strain is small for most target pressures, however, large error can be seen in the third scaffold for E30 at 0.2 bar. This is due to the ballooning phenomenon at higher pressures. More target pressures could be added in the ballooning range to allow more time for the membrane to react to the change in pressure and decrease dynamic affects. A dynamic study should also be carried out in future and compared to the results presented as this could allow faster frequency regimes to be implemented for more varied stimulation methods.

Figure 6 shows the results for varying pre-applied strain to an E50 scaffold. As the pre-applied strain is increased, the strain induced by the stimulating balloon reduces. This can be used to inform more advanced stimulation regimes by combining the modalities of both the stimulating balloon and current robotic bioreactor. The maximum strain achieved with the pre-applied 0, 5, 10 and 20% strains were 47, 42, 37 and 30% respectively. The sum of the maximum strain and the pre-applied strain are similar for each trial. This highlights the region where the actuator is no longer able to apply significant additional strain with increasing pressure.

4 Conclusion

This work presents the design and characterization of a stimulating balloon to increase the modalities of a robotic bioreactor presented in previous works [20]. These preliminary results show that the balloon is capable of providing a large range of tensile strains for scaffolds with varying stiffness. This information could be used for strain-based pressure control during in vitro experiments to follow stimulation regimes. The strain has been considered to act in one direction. By tracking more nodes to the scaffold, the local strain distribution could be better understood. This work could be further used as a building block to explore different configurations of balloons, for example, using an array and comparing how this affects the strain distribution of a tissue construct. Future in vitro experiments will be carried out to further develop this tissue engineering tool and combine the stimulation modalities of the bioreactor. As the stiffness of the tissue changes in real time, tensile testing of the scaffold can be carried out to adapt the pressure control of the stimulating balloon to apply the desired strain. Combined stimulation regimes could be investigated by using the relationship for pressure and strain at different initial strains discussed in this study.

Acknowledgements The authors would like to thank Marco Pontin and Joanna Jones for their input into this work.

References

1. B. Lohberger, H. Kaltenegger, N. Stuendl, B. Rinner, A. Leithner, and P. Sadoghi, "Impact of cyclic mechanical stimulation on the expression of extracellular matrix proteins in human primary rotator cuff fibroblasts," *Knee Surgery, Sports Traumatology, Arthroscopy*, vol. 24, no. 12, pp. 3884–3891, 2016.
2. J. Thanarak, H. Mohammed, S. Pashneh-Tala, F. Claeyssens, and N. Green, "Enhanced collagen production from human dermal fibroblasts on poly (glycerol sebacate)-methacrylate scaffolds," in *2018 11th Biomedical Engineering International Conference (BMEiCON)*. IEEE, 2018, pp. 1–4.
3. J. K. Lee, L. W. Huwe, N. Paschos, A. Aryaei, C. A. Gegg, J. C. Hu, and K. A. Athanasiou, "Tension stimulation drives tissue formation in scaffold-free systems," *Nature Materials*, vol. 16, no. 8, pp. 864–873, 2017.
4. J. Dewey, C. F., S. R. Bussolari, J. Gimbrone, M. A., and P. F. Davies, "The Dynamic Response of Vascular Endothelial Cells to Fluid Shear Stress," *Journal of Biomechanical Engineering*, vol. 103, no. 3, pp. 177–185, 08 1981. [Online]. Available: https://doi.org/10.1115/1.3138276
5. J. Xu, M. Liu, J. Liu, I. Caniggia, and M. Post, "Mechanical strain induces constitutive and regulated secretion of glycosaminoglycans and proteoglycans in fetal lung cells," *Journal of Cell Science*, vol. 109, no. 6, pp. 1605–1613, 06 1996. [Online]. Available: https://doi.org/10.1242/jcs.109.6.1605
6. M. Shachar, N. Benishti, and S. Cohen, "Effects of mechanical stimulation induced by compression and medium perfusion on cardiac tissue engineering," *Biotechnology Progress*, vol. 28, no. 6, pp. 1551–1559, 2012. [Online]. Available: https://aiche.onlinelibrary.wiley.com/doi/abs/10.1002/btpr.1633
7. Tc-3 bioreactor. [Online]. Available: https://ebersmedical.com/tissue-engineering/bioreactors/load-culture/tc-3
8. Biotense bioreactor. [Online]. Available: https://www.admet.com/products/micro-testers/biotense-bioreactor/
9. Cartigen: Mechanical compression bioreactor systems. [Online]. Available: http://www.tissuegrowth.com/prod_cartilage.cfm
10. D. E. Discher, P. Janmey, and Y. L. Wang, "Tissue cells feel and respond to the stiffness of their substrate," *Science*, vol. 310, no. 5751, pp. 1139–1143, 2005.
11. K. Ghosh, Z. Pan, E. Guan, S. Ge, Y. Liu, T. Nakamura, X.-D. Ren, M. Rafailovich, and R. A. Clark, "Cell adaptation to a physiologically relevant ecm mimic with different viscoelastic properties," *Biomaterials*, vol. 28, no. 4, pp. 671–679, 2007.
12. E. Perez Guagnelli, S. Nejus, J. Yu, S. Miyashita, Y. Liu, and D. Damian, "Axially and radially expandable modular helical soft actuator for robotic implantables," 01 2018.
13. S. Todros, S. Spadoni, E. Maghin, M. Piccoli, and P. G. Pavan, "A novel bioreactor for the mechanical stimulation of clinically relevant scaffolds for muscle tissue engineering purposes," *Processes*, vol. 9, 3 2021.
14. J. Paek, J. W. Song, E. Ban, Y. Morimitsu, C. O. Osuji, V. B. Shenoy, and D. D. Huh, "Soft robotic constrictor for in vitro modeling of dynamic tissue compression," *Scientific Reports*, vol. 11, 12 2021.
15. S. C. Carreira, M. Taghavi, E. P. Loriè, and J. Rossiter, "Flexert: A soft, actuatable multiwell plate insert for cell culture under stretch," *ACS Biomaterials Science and Engineering*, vol. 7, pp. 2225–2245, 6 2021.
16. H. Liu, L. A. MacQueen, J. F. Usprech, H. Maleki, K. L. Sider, M. G. Doyle, Y. Sun, and C. A. Simmons, "Microdevice arrays with

strain sensors for 3d mechanical stimulation and monitoring of engineered tissues," *Biomaterials*, vol. 172, pp. 30–40, 2018. [Online]. Available: https://www.sciencedirect.com/science/article/pii/S0142961218303041

17. H. Liu, J. F. Usprech, P. K. Parameshwar, Y. Sun, and C. A. Simmons, "Combinatorial screen of dynamic mechanical stimuli for predictive control of msc mechano-responsiveness," *Science Advances*, vol. 7, no. 19, p. eabe7204, 2021. [Online]. Available: https://www.science.org/doi/abs/10.1126/sciadv.abe7204
18. Tension cell stretching bioreactor system. [Online]. Available: https://www.flexcellint.com/category/tension
19. Y. Kamotani, T. Bersano-Begey, N. Kato, Y. C. Tung, D. Huh, J. W. Song, and S. Takayama, "Individually programmable cell stretching microwell arrays actuated by a braille display," *Biomaterials*, vol. 29, pp. 2646–2655, 6 2008.
20. A. F. Smith, J. Thanarak, M. Pontin, N. H. Green, and D. D. Damian, "Design and development of a robotic bioreactor for in vitro tissue engineering," in *2021 IEEE International Conference on Robotics and Automation (ICRA)*, 2021, pp. 12 428–12 434.
21. E. Luis, H. M. Pan, S. L. Sing, R. Bajpai, J. Song, and W. Y. Yeong, "3d direct printing of silicone meniscus implant using a novel heat-cured extrusion-based printer," *Polymers*, vol. 12, no. 5, 2020. [Online]. Available: https://www.mdpi.com/2073-4360/12/5/1031